A functional link between the actin cytoskeleton and lipid rafts during budding of filamentous influenza virions

Virology **301,** 212–225 (2002)
doi:10.1006/viro.2002.1595

A Functional Link between the Actin Cytoskeleton and Lipid Rafts during Budding of Filamentous Influenza Virions

Martha Simpson-Holley,*[,1] Darren Ellis,*[,†] Dawn Fisher,* Debra Elton,* John McCauley,*[,‡] and Paul Digard*[,2]

*Division of Virology, Department of Pathology, University of Cambridge, Tennis Court Road, Cambridge CB2 1QP, United Kingdom; †Department of Pharmacology, University of Cambridge, Tennis Court Road, Cambridge CB2 1QJ, United Kingdom; and ‡Institute for Animal Health, Compton, Newbury, Berks RG20 7NN, United Kingdom

Received March 13, 2002; returned to author for revision May 1, 2002; accepted May 31, 2002

Morphogenesis of influenza virus is a poorly understood process that produces two types of enveloped virion: ~100-nm spheres and similar diameter filaments that reach 20 μm in length. Spherical particles assemble at plasma membrane lipid rafts in a process independent of microfilaments. The budding site of filamentous virions is hitherto uncharacterised but their formation involves the actin cytoskeleton. We confirm microfilament involvement in filamentous budding and show that after disruption of cortical actin by jasplakinolide, HA, NP, and M1 redistributed around β-actin clusters to form novel annular membrane structures. HA in filamentous virions and jasplakinolide-induced annuli was detergent insoluble at 4°C. Furthermore, in both cases HA partitioned into low buoyant density detergent-insoluble glycolipid domains, indicating that filamentous virions and annuli contain reorganised lipid rafts. We propose that the actin cytoskeleton is required to maintain the correct organisation of lipid rafts for incorporation into budding viral filaments.

Key Words: cytochalasin D; latrunculin A; atomic force microscopy.

INTRODUCTION

Influenza virions are enveloped by a host-derived lipid bilayer containing three viral proteins, the haemagglutinin [HA] and neuraminidase [NA] glycoproteins, involved in entry and exit, and the M2 ion channel, which plays a role in viral uncoating (Lamb and Krug, 1996). The viral envelope surrounds a shell of matrix protein (M1), within which lie the internal genomic ribonucleoprotein (RNP) particles. Each RNP consists of one of the eight negative-sense viral RNA segments encapsidated by nucleoprotein (NP) and one copy of the trimeric viral polymerase (Portela and Digard, 2002). In addition, virion cores contain a low abundance NEP/NS2 polypeptide, thought to play a role in export of the RNPs from the cell nucleus, the site of viral transcription (O'Neill *et al.,* 1998).

Virions are formed by budding from the apical surface of the plasma membrane in infected epithelial cells (Bachi *et al.,* 1969; Rindler *et al.,* 1985). Thus the virus must assemble its structural components within an area of the plasma membrane which can pinch off to form a particle of around 100 nm diameter. Historically, it has been postulated that influenza viral glycoproteins might localise other viral components to budding domains in the plasma membrane (Compans and Choppin, 1975). In support of this hypothesis, there is evidence for interactions between M1 and the cytoplasmic tails of the HA and NA glycoproteins (Enami and Enami, 1996; Jin *et al.,* 1997; Ali *et al.,* 2000; Zhang *et al.,* 2000) and for M1-RNP interactions (Zvonarjev and Ghendon, 1980; Martin and Helenius, 1991; Zhang and Lamb, 1996; Ye *et al.,* 1999). Furthermore, the advent of the lipid raft model of membrane structure provides a possible mechanism for the concentration of the viral glycoproteins and thus the internal components into localised regions for efficient budding. The lipid raft model states that certain species of saturated lipid (glycosphingolipids and sphingomyelin), along with cholesterol, preferentially associate with one another to form ordered domains in the plasma membrane that incorporate a specific subset of membrane proteins (Brown and Rose, 1992; Simons and Ikonen, 1997; Brown and London, 1998). Lipid rafts have been defined primarily by biochemical means, particularly their insolubility in nonionic detergents at low temperatures (Brown and Rose, 1992; Fiedler *et al.,* 1993). Their visual definition has been more problematic, although single-particle tracking and fluorescent resonance energy transfer methods suggest that they are generally small structures on the scale of ≈100 nm (Kenworthy and Edidin, 1998; Varma and Mayor, 1998; Pralle *et al.,* 2000; Schutz *et al.,* 2000; reviewed by Jacobson and Dietrich, 1999). Thus, lipid rafts might facilitate the concentration of viral components into suitably sized budding domains in the plasma membrane. Indeed, both

[1] Present address: Department of Pathobiology, School of Veterinary Medicine, University of Pennsylvania, 3800 Spruce Street, Philadelphia, PA 19104-6049.

[2] To whom correspondence and reprint requests should be addressed. Fax: +44 1223 336926. E-mail: pd1@mole.bio.cam.ac.uk.

0042-6822/02 $35.00

HA and NA are incorporated into lipid rafts (Scheiffele *et al.,* 1997, 1999; Barman and Nayak, 2000), and furthermore, virus particles from the fowl plague A/FPV/34 (FPV; H7N1) and A/WSN/33 (WSN; reassorted to H3N1) strains have been shown to bud from rafts and contain raft-incorporated lipids (Van Meer and Simons, 1982; Scheiffele *et al.,* 1999; Zhang *et al.,* 2000). It has also been proposed that host cell membrane proteins are excluded from budding influenza viruses (Compans and Choppin, 1975; Naim and Roth, 1993). Such selectivity could be exerted at least in part through discrimination between raft-associated and nonraft proteins. Thus virus exploitation of the lipid raft system potentially provides an intrinsic mechanism for the concentration of viral proteins and the exclusion of a large proportion of cellular proteins from viral budding sites (Zhang *et al.,* 2000).

The morphology of influenza virions varies considerably. Laboratory-adapted influenza virus strains generally produce pleomorphic, approximately spherical particles with a diameter of 80–120 nm (Ruigrok *et al.,* 1985; Jin *et al.,* 1997). However, in addition to spherical particles, certain strains of influenza virus also produce large numbers of virions with a filamentous morphology (Mosley and Wyckoff, 1946; Chu *et al.,* 1949; Choppin *et al.,* 1960) and there is evidence that filamentous forms might be present *in vivo* in the human host (Chu *et al.,* 1949). Filamentous virions have similar diameters to spherical particles (~100 nm), but are vastly elongated; in the case of the A/Udorn/72 (Udorn; H3N2) strain virus particles reach lengths of up to 30 μm (Roberts and Compans, 1998). Thus, although spherical virions can be considered to be comparably sized to their putative lipid raft budding site, filamentous virions are substantially larger. Genetic factors affect virion shape: the matrix genes, HA, and NA are significant in determining filament formation (Smirnov, 1991; Roberts *et al.,* 1998). However, host cell factors also play a role, and in particular, the sensitivity of filamentous (but not spherical) virus budding to cytochalasin D, an inhibitor of actin polymerization, suggests that their formation depends on an intact actin cytoskeleton (Roberts and Compans, 1998). The precise role of actin in assembly of filamentous morphology virions is unknown, but unlike other viruses such as measles (Bohn *et al.,* 1987), actin has not been found inside influenza virions or budding particles. Although an intact actin cytoskeleton is not essential for the assembly of spherical virus particles (Griffin and Compans, 1979; Roberts and Compans, 1998), there is evidence suggesting that a fraction of the RNPs and M1 protein in infected cells is associated with microfilaments (Avalos *et al.,* 1997; Husain and Gupta, 1997) and NP has been shown to be an F-actin binding protein (Digard *et al.,* 1999, 2001).

The experiments described here were carried out to investigate further the role of the cytoskeleton in the formation of filamentous influenza virus particles and to examine whether filamentous virion assembly involves lipid rafts. Three drugs which disrupt actin treadmilling in mechanistically distinct ways inhibited filamentous virion production. Furthermore, drug treatment led to the specific reorganisation of HA, M1, and RNP into a previously unrecognised annular cell-surface structure formed around a core of aggregated β-actin underlying the plasma membrane. Filamentous virions and HA annuli were resistant to low temperature detergent extraction and the HA of Udorn virus was incorporated into low buoyant density detergent-insoluble glycolipid domains (DIGs), indicating that filamentous influenza virions bud from lipid raft domains. We therefore suggest that the dependence of filamentous virion assembly on the microfilament network reflects a raft–actin interaction that maintains the necessary organisation of HA-containing lipid rafts for their incorporation into budding particles.

RESULTS

Filamentous virion assembly and HA distribution on the cell surface are affected by disruption of the actin cytoskeleton

Previous work has shown that cytochalasin D inhibits the production of filamentous but not spherical virions by the Udorn virus, suggesting a specific requirement for the actin cytoskeleton in the assembly of filamentous particles (Roberts and Compans, 1998). To test further the relevance of the actin cytoskeleton to virion assembly, we examined the effects of a mechanistically different inhibitor of actin treadmilling on influenza virus infection. Cytochalasin D prevents actin polymerisation by binding to the barbed ends of actin filaments and blocking the addition of soluble (G)-actin monomers (Schliwa, 1982). We therefore tested the effects of jasplakinolide, a drug which binds to F-actin and inhibits actin depolymerization (Bubb *et al.,* 1994) on the replication of Udorn and A/PR/8/34 (PR8; H1N1), as representative filamentous and nonfilamentous viruses, respectively. Polarized epithelial Madin–Darby canine kidney (MDCK) cells were infected or mock-infected with each virus for 1 h at 37°C and then incubated in the presence or absence of varying concentrations of jasplakinolide. At 8 h p.i., cell supernatants were collected and the titre of released virus measured by plaque assay, while the infected cells were fixed and examined by fluorescent microscopy for cell-surface HA and internal actin. The lowest dose of drug tested (0.3 μM) was sufficient to cause marked clumping of the cortical actin web, while higher doses caused complete collapse of the actin cytoskeleton and rounding and aborization of the cells (data not shown, but see Fig. 2). However, no reduction in virus titre was seen at any concentration of drug for either virus (Table 1). In replicate experiments, even the highest concentration of drug tested (3 μM) did not reduce the release of infectious Udorn virus, as titres in the absence of drug were $6.3 \pm 3.4 \times 10^6$ PFU/ml compared to $5.7 \pm 1.1 \times 10^6$

TABLE 1

Effect of Actin-Binding Drugs on Influenza Virus Replication

Drug	% Titre in absence of drug	
	A/Udorn/72	A/PR/8/34
Jasplakinolide (μM)		
0.3	160	150
1.0	100	180
3.0	340	130
Latrunculin A (nM)		
0.2	109	
0.6	100	
1.7	155	
5	173	

MDCK cells were infected with influenza viruses in the presence of drugs as indicated and released titres at 8 h p.i. measured on MDCK cells. Values are expressed as the percentage of titres obtained in the presence of the drug solvent, DMSO. 100% values for A/Udorn/72 ranged between 1.1 and 1.5 $\times$ 10^6 pfu/ml, while those for A/PR/8/34 were 5 $\times$ 10^7 pfu/ml.

PFU/ml in the presence of drug (n = 4). The apparent failure of the drugs to inhibit virus replication was not an artifact arising from carryover of input virus because parallel experiments using other drugs such as leptomycin B (Elton *et al.,* 2001) or methyl-β-cyclodextrin (data not shown) did show reduced titres of released virus. Consistent with the lack of effect on virus release, parallel analysis of polypeptide synthesis by metabolic labelling or Western blot showed no discernible effects of jasplakinolide treatment on viral protein synthesis (data not shown). Mock-infected, HA-stained samples showed low levels of nonspecific antibody binding (Fig. 1f and data not shown). In the absence of jasplakinolide, Udorn infection produced distinctive HA-stained filamentous structures on the cell surface, which reached several microns in length (Fig. 1a). In contrast, PR8 infection produced a stippled staining pattern, with HA distributed irregularly over the cell surface (Fig. 1d). The differing HA distributions reflect the very different budding strategies of the two viruses. In the presence of jasplakinolide, Udorn infection no longer produced filamentous virions and instead, HA was found clumped into ring-shaped domains distributed across the surface of the cell (Fig. 1b). Under higher power magnification these domains were seen in many cases to show a clear annular structure (Fig. 1c, top). These annuli of HA were distinctive in shape and distribution and their size was found to be regular (1.8 $\pm$ 0.3 μm in diameter, n = 99, two independent experiments). When data from confocal microscopy was used to recreate a cross-sectional view from serial optical planes of focus, the annuli appeared as hemi-

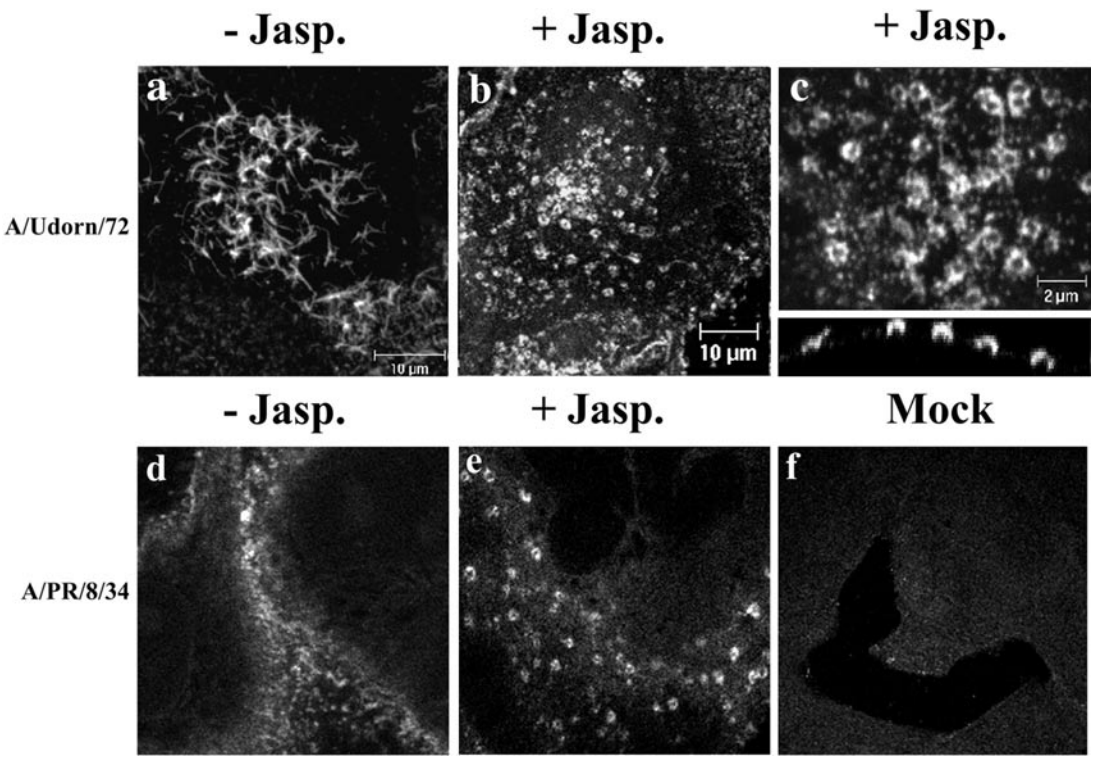

FIG. 1. Effect of jasplakinolide treatment on the distribution of cell surface HA in influenza virus infected cells. MDCK cells were mock infected (f) or infected (a–e) with the Udorn (a–c) or PR8 (d–e) strains of influenza virus and in certain cases incubated with 0.3 μM jasplakinolide (+Jasp) as indicated. 8 h p.i. cells were fixed, stained for cell surface HA, and imaged by confocal microscopy. Extended focus projections are shown, except for the lower portion of (c), which shows a z-axis reconstruction.

spherical protrusions from the surface of the plasma membrane (Fig. 1c, bottom). The formation of these annuli was not peculiar to the filamentous virus as similar domains were observed in drug-treated, PR8-infected cells (Fig. 1e). The rings of PR8 HA observed in cells treated with jasplakinolide were of a similar size and distribution to those seen in cells infected with Udorn. Thus inhibition of actin depolymerization as well as polymerisation blocks the assembly of filamentous influenza virions without decreasing the overall titre of released virus. Furthermore, jasplakinolide treatment leads to the specific reorganisation of cell-surface HA into annular aggregations irrespective of whether the virus strain normally produces spherical particles only, or a mixture of filamentous and spherical particles.

Treatment of cells with jasplakinolide leads to specific changes in the distribution of HA. It was therefore of interest to determine the nature of the disruption to the actin cytoskeleton which was responsible for these changes. Accordingly, we examined whether actin and cell-surface HA colocalised in Udorn-infected cells with and without jasplakinolide treatment. To detect actin we used either a monoclonal antibody specific for the β-actin isoform or a fluorescently tagged phalloidin as a general probe for F-actin. As expected, β-actin in untreated cells was distributed as a layer of cortical actin underlying the plasma membrane (Fig. 2a, ii). Counterstaining for HA showed viral filaments budding from the plasma membrane, often in arrays in close proximity to the underlying β-actin (Fig. 2a, i, iii). However, no evidence for significant incorporation of actin into the viral filaments was observed (Fig. 2a and data not shown). In drug-treated cells, surface HA was again reorganised into the characteristic annular structures distributed across the cell surface (Fig. 2a, iv). Staining for β-actin in drug-treated cells showed complete loss of the cortical actin web with the actin instead aggregated into discrete clumps distributed across the cell (Fig. 2a, v). Strikingly, each focal cluster of β-actin was located in the center of a cell-surface annulus of HA (Fig. 2a, vi). *z*-Axis reconstructions showed that the aggregations of actin were positioned just below the plasma membrane underneath and partially inside the surrounding rings of viral HA (Fig. 2b). When infected, drug-treated cells were stained with fluorescent phalloidin, a similar array of punctate spots of F-actin were seen (Fig. 2c, ii), although interestingly, under these conditions the network of basement stress fibres was largely intact (data not shown). Moreover, high-power magnification showed that each punctate focus of F-actin was at the center of an annulus of cell-surface HA and that although the segregation of the two proteins was clearly linked, there was very little direct colocalisation of the two fluorophores (Fig. 2c, i, iii). Thus the redistribution of cell-surface HA after jasplakinolide treatment is accompanied by a matching reorganisation of the underlying actin cytoskeleton.

Jasplakinolide and cytochalasin D disrupt the actin cytoskeleton by different mechanisms and yet both inhibit the assembly of filamentous influenza virions. In the case of jasplakinolide treatment, the collapse of the cortical actin web is associated with a corresponding reorganisation of cell-surface HA into annuli. We therefore tested if this phenomenon was unique to jasplakinolide or whether other actin-disrupting drugs also caused HA reorganisation. MDCK cells were infected with Udorn and treated 1 h p.i. with latrunculin A or cytochalasin D. Latrunculin A inhibits actin polymerisation by sequestering G-actin monomers and thus disrupts the actin treadmilling cycle in a mechanistically distinct way from cytochalasin D and jasplakinolide (Coue *et al.,* 1987). At 8 h p.i., cells were fixed and stained for F-actin and HA. Very few viral filaments were visible in cells treated with latrunculin A; instead cell-surface HA was clumped into aggregations, often ring-shaped (Fig. 3a). The rings of HA observed in latrunculin A treated cells were of a similar size to those observed in the presence of jasplakinolide (around 1.5 μm diameter). Also similarly to jasplakinolide, latrunculin A induced the formation of punctate aggregations of F-actin which coincided with the centre of the HA aggregations (Figs. 3b and 3c). In addition, when the titres of released virus were measured, there was no apparent reduction in virus replication across a range of latrunculin A concentrations (Table 1), implying that spherical particle production was unaffected. Next, we tested the effects of cytochalasin D and found that as previously reported (Roberts and Compans, 1998), it disrupted filament formation by Udorn (Fig. 3d). Furthermore, after drug treatment, the viral HA formed clumps which colocalised with punctate aggregations of F-actin, although neither the actin foci or the corresponding HA reorganisation was as distinct as with the other two inhibitors (Figs. 3e and 3f). Thus, three drugs which disrupt the actin treadmilling cycle in different ways induce the formation of punctate aggregations of F-actin and prevent the assembly of long filamentous virions, without any apparent inhibitory effect on overall virus replication. Furthermore, in each case the collapse of the cortical actin web is accompanied by a matching rearrangement of cell-surface HA into distinctive, often annular aggregations.

Scanning electron microscopy (SEM), atomic force microscopy (AFM), and transmission electron microscopy (TEM) were used to study the morphology of the annular domains formed after actin disruption. MDCK cells were infected with Udorn and then incubated in the presence or absence of jasplakinolide. At 8 h p.i., cells were fixed and prepared for microscopy. In the absence of drug, SEM showed virus filaments measuring several microns in length on the surface of infected cells (Fig. 4a). Microvilli were also observed, distributed evenly across the cell surface. In the presence of jasplakinolide, long viral filaments were greatly reduced in number but clumps of

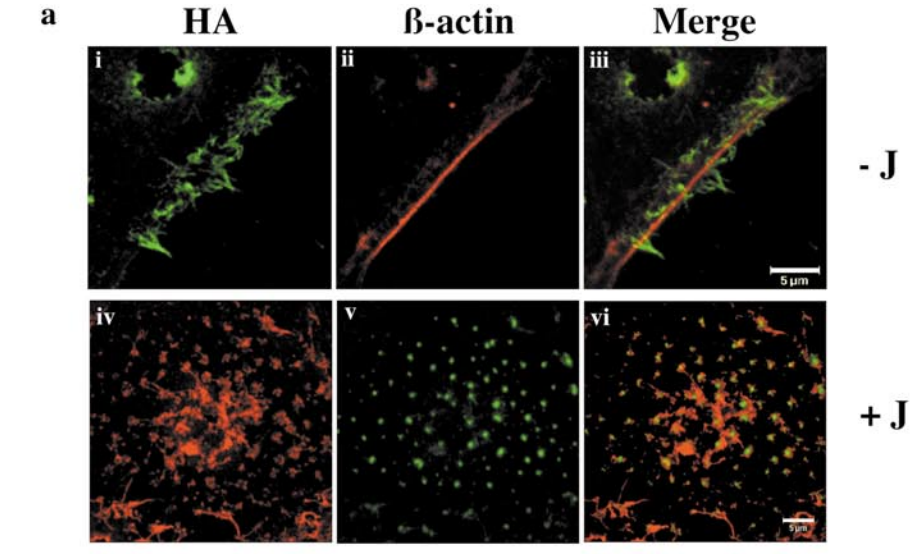
a
HA
ß-actin
Merge
i
ii
iii
- J
5 µm
iv
v
vi
+ J
5 µm

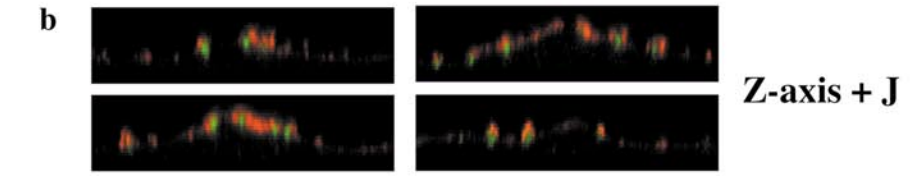
b
Z-axis + J

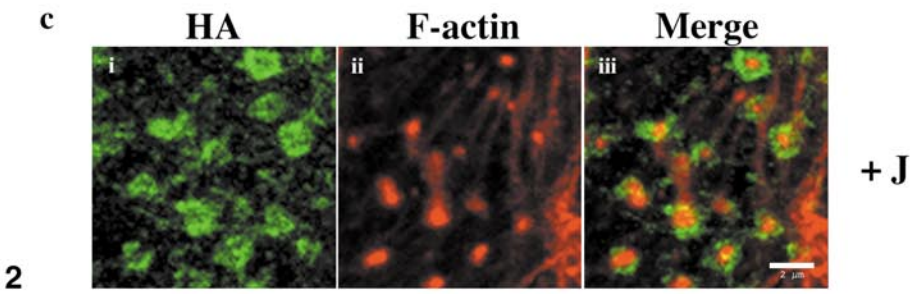
c
HA
F-actin
Merge
i
ii
iii
+ J
2 µm

2

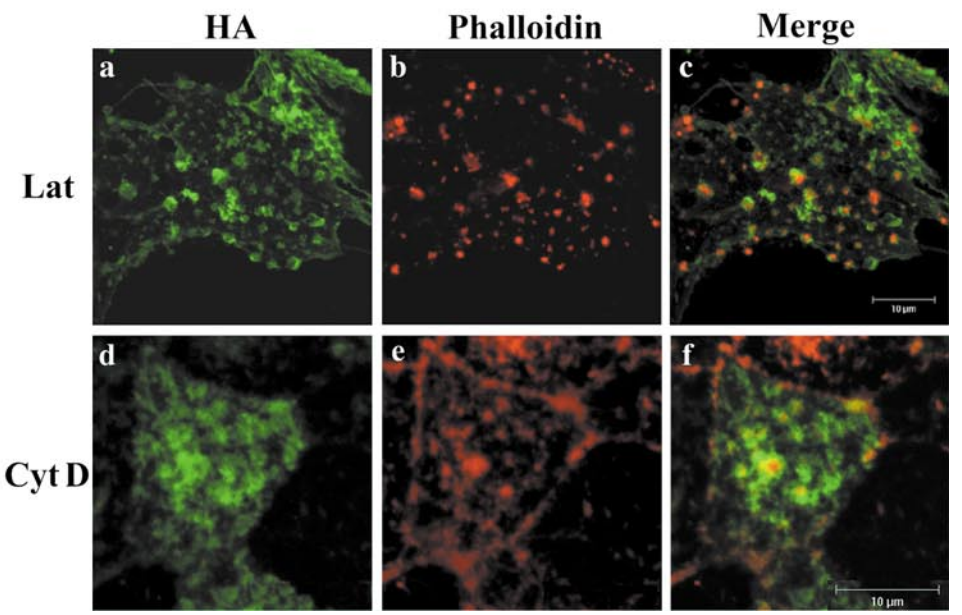
HA
Phalloidin
Merge
Lat
a
b
c
10 µm
Cyt D
d
e
f
10 µm

3

short filaments were observed, distributed across the cell surface (Fig. 4b). Closer examination of these structures showed short filaments apparently radiating from a focal point, with an overall diameter of 1–2 μM (Fig. 4b, inset). The occasional longer filamentous structure observed in drug-treated cells originated from these clumps of short filaments. AFM imaging also showed virus filaments several microns in length budding from the surfaces and edges of infected cells incubated in the absence of drug (Fig. 4c). In addition, the filaments were often organised in parallel bundles (Fig. 4c, ii). In the presence of jasplakinolide, clumps of filaments strikingly similar to those observed using SEM were seen (Fig. 4d). Again, these domains were roughly circular and resembled short filaments radiating from a central point. TEM imaging of infected cells in the absence of drug treatment showed the presence of a mixture of short and long filamentous structures close to or actually budding from the plasma membrane (Fig. 4g, arrows) as well as apparently spherical virus particles (Fig. 4e, arrows). However, after jasplakinolide treatment, no long filaments were visible and the cell surfaces were instead decorated with a mixture of short filaments and numerous spherical virus particles (Figs. 4f and 4h). In addition, the short filaments that were apparently attached to the plasma membrane often appeared to be clumped (Fig. 4f, arrows), consistent with the three-dimensional SEM and AFM images. Thus jasplakinolide-induced actin disruption leads to physical alteration of the surface structure of the plasma membrane without preventing the assembly and release of spherical influenza virions. We conclude that the drug-induced aggregations of short filamentous structures most likely correspond to the rings of HA seen by confocal immunofluorescence microscopy.

The intracellular viral components M1 and NP redistribute with HA in response to actin disruption

Destruction of the cortical actin web inhibited the formation of long viral filaments and led to reorganisation of cell-surface HA (Figs. 1–4) but did not decrease the overall titre of released spherical virions (Table 1). Therefore it seemed possible that the rings of cell-surface HA corresponded to reorganised viral budding sites. To test this hypothesis, we examined whether the subcellular distribution of the major internal components of the virion altered in response to jasplakinolide treatment. MDCK cells were infected with Udorn virus, incubated in the presence or absence of jasplakinolide, permeabilised 8 h p.i. using 1% TX-100 at 4°C, and then fixed and examined by confocal microscopy after staining for NP. In the absence of the drug, RNP staining showed filamentous viral structures, while mock-infected cells showed very little staining (Figs. 5c and 5d). In jasplakinolide-treated cells filaments were not seen; instead aggregations of RNP were observed (Fig. 5a), which under higher power magnification showed distinct circular patterns (Fig. 5b). These rings of RNP were of a similar diameter to those observed previously for HA (around 1.5 μm).

Next, we examined the distribution of M1. To permit noninvasive tracking of M1 and to allow colocalisation studies with HA, we utilised an M1-green fluorescent protein (GFP-M1) fusion. MDCK cells were transfected with plasmid pGFPM703 encoding a GFP-M1 fusion protein under the control of a cytomegalovirus immediate early promoter (or with plasmid pEGFP-c2 expressing GFP alone) and 18 h later, some cultures were superinfected with Udorn and treated with jasplakinolide. At 8 h p.i., the cells were fixed, stained for cell-surface HA, and examined by confocal microscopy. In the absence of drug in infected cells, both GFP-M1 and GFP (data not shown) showed a mixture of nuclear and cytoplasmic accumulation, consistent with the presence of a nuclear localisation signal in M1 (Ye *et al.,* 1995) and the ability of nonfused GFP to transfer passively into the nucleus because of its relatively small size. However, while GFP alone displayed diffuse cytoplasmic localisation, a substantial proportion of the cytoplasmic GFP-M1 was in the form of filamentous structures (Fig. 6a, ii). When the surface distribution of HA was examined, pGFPM703-transfected cells displayed numerous viral filaments (Fig. 6a, i) and these HA-containing structures colocalized with those of the GFP-tagged M1 in merged images (Fig. 6a, iii), indicating incorporation of GFP-M1 into viral filaments. *z*-Axis reconstructions of bundles of viral filaments projecting away from the surface of infected cells showed marked colocalisation of HA and GFP-M1 (Fig. 6b, i), but no detectable incorporation of GFP alone (Fig. 6b, ii), confirming that GFP-M1 was specifically incorpo-

FIG. 2. Jasplakinolide induced collapse of the cortical actin web leads to matching changes in cell-surface HA distribution. MDCK cells were infected with Udorn virus and treated with 0.3 μM jasplakinolide (+J) or left untreated (−J) as before, fixed at 8 h p.i., and examined by fluorescent staining and confocal microscopy for the distribution and codistribution (merged images) of HA and β-actin as indicated using the appropriate antibodies (a, b), or F-actin using Alexa-594-conjugated phalloidin (c). Images are extended focus projections except for those in (b) which are *z*-axis reconstructions.

FIG. 3. Mechanistically different inhibitors of actin treadmilling cause the formation of punctate spots of F-actin surrounded by clumps of cell surface HA. MDCK cells were infected with Udorn virus and treated from 1 h p.i. with 3 nM latrunculin A (a–c) or 0.5 μg/ml cytochalasin D (d–f). At 8 h p.i. cells were fixed and stained for HA and F-actin using fluorescently labelled phalloidin (as labelled) and examined by confocal microscopy. Extended focus projections are shown.

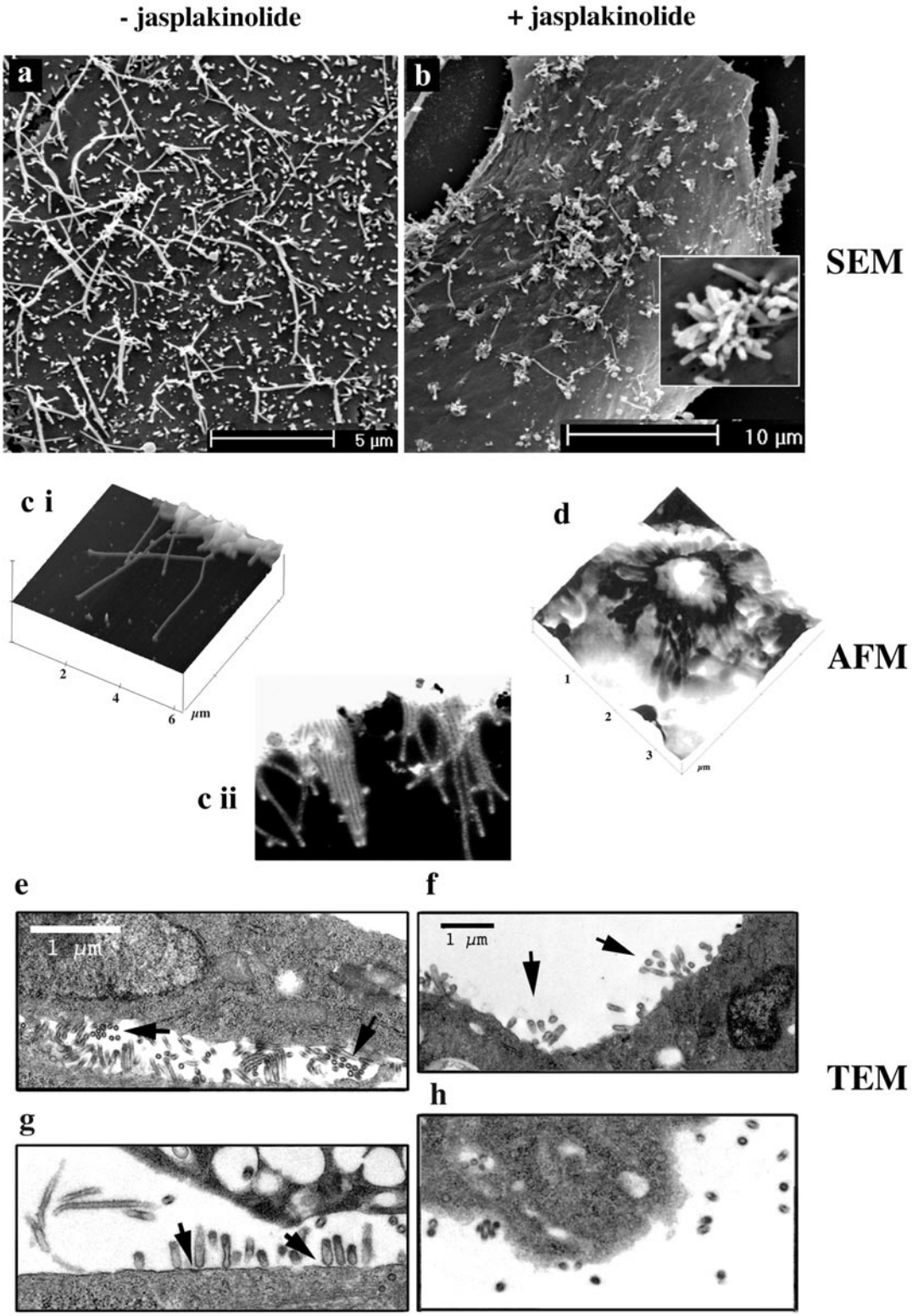

FIG. 4. Physical features of the surface of Udorn infected cells. MDCK cells were infected with Udorn virus and incubated in the presence (b, d, f, h) or absence (a, c, e, g) of 0.3 μM jasplakinolide. At 8 h p.i. cells were fixed and imaged by SEM (a, b), AFM (c, d), or TEM (e–h). Arrows indicate (e) clusters of apparently spherical virus particles; (f) possible clusters of short filaments; (g) virus particles in close proximity to the plasma membrane, possibly in the process of pinching-off.

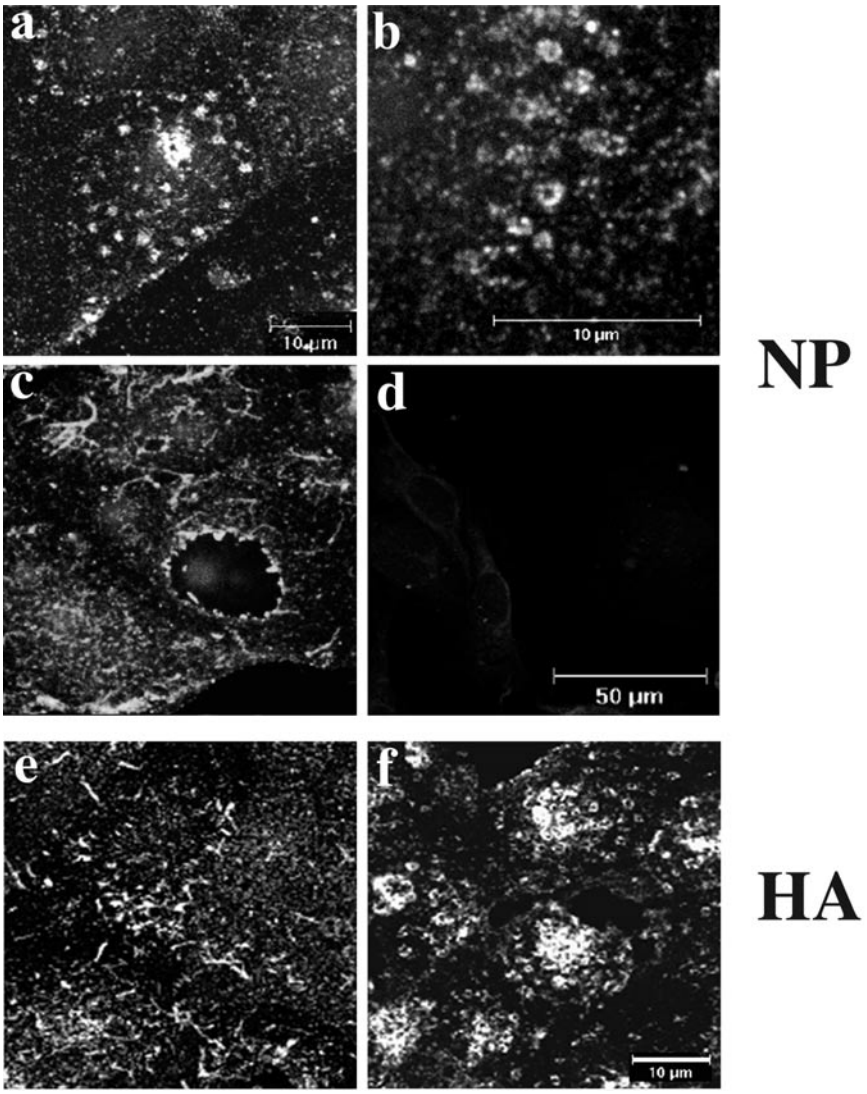

FIG. 5. RNP and HA distribution in detergent-extracted cells. MDCK cells were infected (or mock infected; d) with Udorn virus and were either incubated with 0.3 μM jasplakinolide from 1 h p.i. (a, b, f) or left untreated (c–e). At 8 h p.i. cells were extracted on ice with 1% TX-100, fixed, and immunostained for NP (a–d) or HA (e, f). Confocal extended focus projections are shown.

rated into viral filaments. In addition, no large filamentous structures were seen in uninfected cells transfected with pGFPM703 (Fig. 6b, iii). Thus GFP-tagged M1 is competent to interact with wild-type viral components and to be incorporated into budding virions. We therefore went on to examine the effect of jasplakinolide treatment on GFP-M1 localisation in virus-infected cells. In drug-treated cells, surface HA displayed the characteristic annular staining pattern (Fig. 6a, iv). Under these conditions, GFP-M1 was not found in filamentous structures, but was also located in focal aggregates, many of which showed a ring-like appearance and all of which colocalised with the HA annuli (Fig. 6a, v, vi). Under high-power magnification, the two fluorophores were found in close proximity at the nanometer level (Fig. 6a, vii–ix). Thus disruption of the actin cytoskeleton leads to reorganisation of the two major cytosolic components of influenza virions. This supports the hypothesis that the drug-induced annuli of cell-surface HA correspond to reorganised viral budding sites. This is also consistent with the study of Avalos *et al.* (1997), which showed colocalisation of M1 and NP with actin in membrane blebs at the periphery of markedly arborized cells after cytochalasin D treatment.

Filamentous influenza virions are associated with lipid raft structures

Strains of influenza virus which produce solely spherical virions have been shown to exploit lipid raft domains for the purpose of assembly and budding (Scheiffele *et al.,* 1999; Zhang *et al.,* 2000). We therefore tested whether this was the case for the vastly larger virus particles produced by the filamentous Udorn strain and also for

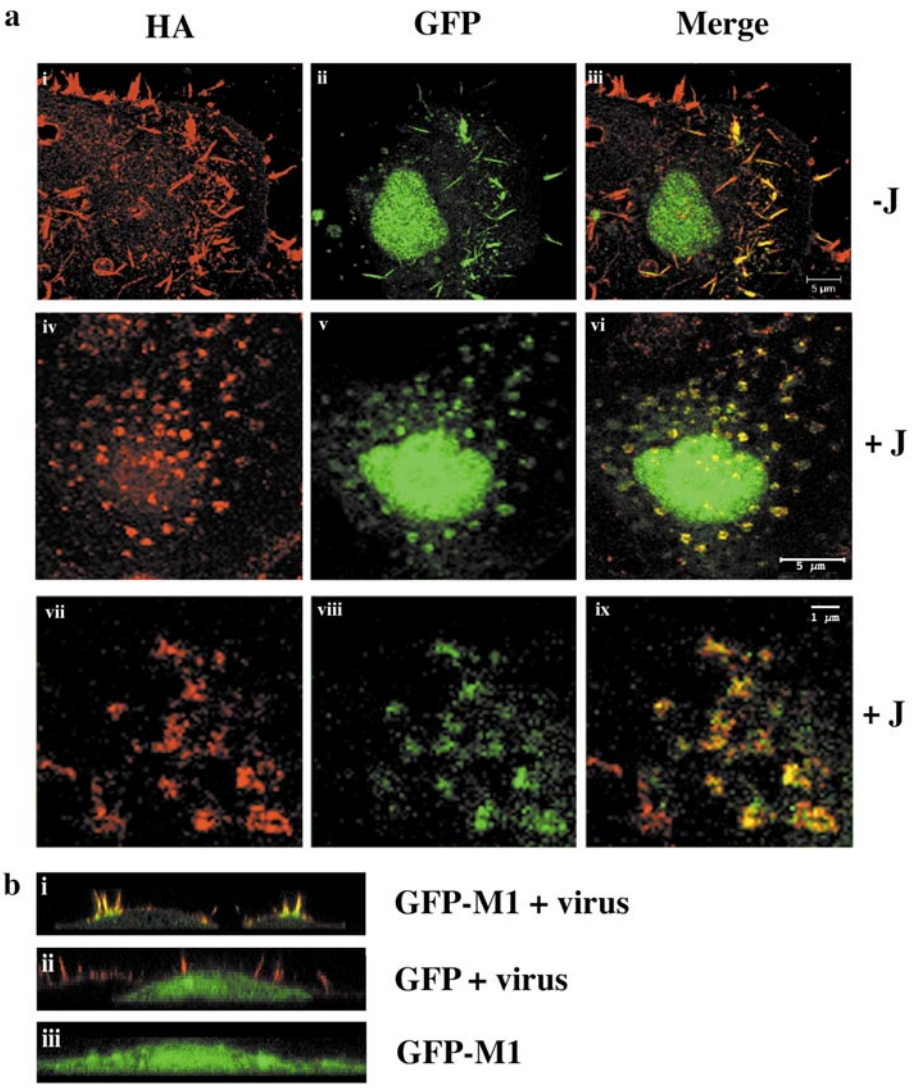

FIG. 6. A GFP-M1 fusion protein is incorporated into budding viral filaments and redistributes in response to actin disruption. MDCK cells were transfected with plasmid pGFPM703 (a, b i, iii) or pEGFP-c2 (b ii), superinfected with A/Udorn/72 (a, b i, ii) or mock-infected (b iii), and incubated in the presence (a iv–ix) or absence (a i–iii; b) of 0.3 μM jasplakinolide from 1 h p.i. At 8 h p.i. cells were fixed, stained for surface HA in red and examined by confocal microscopy for HA and GFP distribution. (a) shows extended focus projections. (b) shows *z*-axis reconstructions of HA and GFP distribution from the indicated combinations of plasmid and virus.

the annular HA structures induced by cytoskeletal disruption. The primary experimental definition of lipid rafts and their associated polypeptides is their insolubility in nonionic detergent at low temperatures (Brown and Rose, 1992; Fiedler *et al.,* 1993). Accordingly, 8 h p.i., Udorn-infected MDCK cells were incubated at 4°C in buffer containing 1% Triton X-100 (TX-100) for 30 min. Cells were then washed, fixed, and examined by confocal microscopy after staining for HA. In the absence of jasplakinolide treatment, filaments incorporating HA were visible that were of a similar length to those seen in experiments where the cells were fixed without prior detergent extraction (Fig. 5e). As before, no viral filaments were observed in drug-treated cells, and instead, HA staining was reorganised into annular domains (Fig. 5f). These had survived detergent extraction and appeared of similar size, intensity, and abundance to those observed in the absence of detergent extraction. Thus, HA in both filamentous virions and drug-induced annuli is resistant to *in situ* extraction with nonionic detergent at 4°C, consistent with its presence in lipid raft domains.

The *in situ* low-temperature detergent insolubility of Udorn HA described above could potentially result not from its incorporation into lipid rafts, but from an association with other insoluble nonmembranous viral and/or cellular structures. To test this possibility, we examined whether the filamentous Udorn HA partitioned into low buoyant density detergent-insoluble glycolipid domains, as has previously been demonstrated for the HAs from the spherical virions produced by the other influenza strains studied (Scheiffele *et al.,* 1999; Zhang *et al.,* 2000). For the purposes of comparison, we also examined the

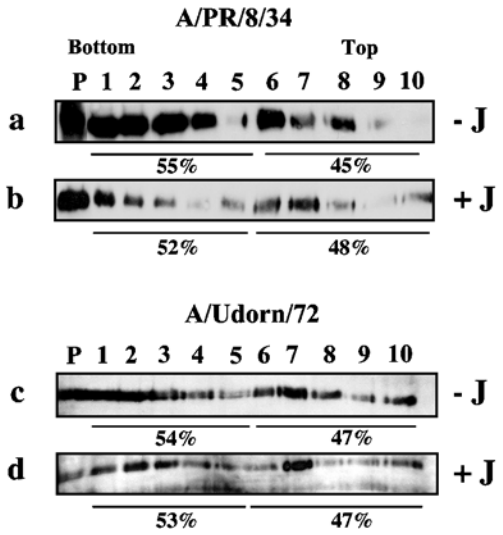

FIG. 7. Sucrose floatation gradient analysis of low temperature detergent extracted cell lysates. MDCK cells were infected with A/PR/8/34 or A/Udorn/72 as indicated and incubated from 1–8 h p.i. in the presence (b, d) or absence (a, c) of 0.3 μM jasplakinolide. Following extraction with TX-100 at 4°C, cells were loaded at the bottom of a sucrose floatation gradient and subjected to centrifugation. Fractions (numbered from the bottom of the gradient) were collected and examined for HA content by Western blot. P = pellet. Percentages show the amounts in the top and bottom halves of the gradient as determined by densitometry.

behaviour of the nonfilamentous PR8 strain HA. MDCK cells were infected with either virus, and at 8 h p.i., extracted in buffer containing 1% TX-100 at 4°C for 30 min. The cell lysates were then adjusted to 40% sucrose (w/v) and loaded at the bottom of a discontinuous sucrose gradient. Following centrifugation, fractions were collected and analysed for HA content by Western blotting. Substantial quantities of the PR8 HA partitioned into the upper part of the sucrose gradient, indicating its association with a detergent insoluble membrane fraction (Fig. 7a). The proportion of HA seen in the upper and lower halves of the gradient was estimated by densitometry. In replicate experiments, 49 $\pm$ 8% (n = 4) of the HA was found in low buoyant density fractions. When cells infected with A/Udorn/72 were studied, the H3 HA behaved similarly to the PR8 HA and partitioned approximately equally between buoyant (45 $\pm$ 12%, n = 4) and nonbuoyant fractions (Fig. 7c). This is consistent with previous results testing the raft association of an A/Udorn/72 HA in a WSN genetic background that does not produce significant numbers of filamentous particles (Zhang *et al.,* 2000). Therefore the HA from a filamentous strain of influenza virus displays a similar degree of association with detergent-insoluble lipid raft structures to the HA from a nonfilamentous strain. Next, we examined whether cytoskeletal disruption (and the accompanying reorganisation of the surface HA) had any effect on the HA-DIG association. When extracts from infected cells incubated in the presence of jasplakinolide were fractionated, neither strain of HA showed any significant change in its degree of DIG association (Figs. 7b and 7d), with 48 $\pm$ 16% (n = 4) and 43 $\pm$ 6% (n = 3) of the PR8 and Udorn HAs, respectively, still partitioning into low buoyant density fractions. Thus the HA in filamentous influenza virions is associated with lipid rafts.

DISCUSSION

Assembly of filamentous influenza virus particles has been proposed to depend on the actin cytoskeleton, based on their sensitivity to the inhibitor of actin polymerisation, cytochalasin D (Roberts and Compans, 1998). Here, this hypothesis was strengthened by testing the effect of drugs which perturb the actin treadmilling cycle through different mechanisms. Jasplakinolide, an inhibitor of actin depolymerisation, and latrunculin A, a G-actin binding drug, were both found to prevent the assembly of filamentous but not spherical virus particles (Figs. 1, 3, 4, and Table 1). Thus the loss of filament production in cytochalasin D treated cells (Roberts and Compans, 1998) is not unique to this drug and does reflect a requirement for the microfilament network. This is noteworthy since the closely related drug cytochalasin B has been shown to inhibit release of influenza virions from infected cells, not by interfering with the assembly process but because cytochalasin B has a unique effect on the glycosylation of the neuraminidase (Griffin and Compans, 1979).

We also show that disruption of the microfilament network leads to the formation of a previously unrecognised annular structure on the surface of infected cells. Physically, this structure consisted of a regularly sized clump of short filaments radiating away from a focal point (Fig. 4). These annuli incorporated HA on the cell exterior, and on the cytoplasmic surface of the plasmamembrane, M1 and RNP, arranged around aggregations of polymerised β-actin (Figs. 2, 5, 6, and 8). Formation of these annuli was most marked following jasplakinolide treatment but could also be observed after treatment with cytochalasin D and latrunculin A (Fig. 3). Cortical aggregations of actin have previously been observed following cytochalasin D and jasplakinolide treatment or microinjection of phalloidin, which acts similarly to jasplakinolide (Wehland *et al.,* 1977; Schliwa, 1982; Bubb *et al.,* 1994, 2000). To our knowledge, however, this is the first time it has been shown that the formation of such structures is accompanied by a matching distinctive reorganisation of membrane-associated proteins. Longer viral filaments were sometimes seen protruding from annuli, an effect that was particularly marked when drug treatment was initiated at 4 h p.i., just prior to the onset of detectable filament production (data not shown). In addition, the effect of jasplakinolide treatment was reversible, since removal of the drug was accompanied by recovery of the cortical actin web, loss of HA annuli, and the resumption of filament production (data not shown).

Thus the formation of annular domains is concomitant with the loss of normal filament assembly. We therefore postulate that as the cortical actin network collapses into punctate aggregations, viral filaments and viral assembly sites are dragged in to surround them. After actin disruption, the spherical virion production that still occurs is likely to take place at the annuli, since HA, M1, and NP accumulate in these domains. This is consistent with the finding that the HA of the PR8 strain of influenza (which only produces spherical particles) also redistributes into annular domains after jasplakinolide treatment (Fig. 1e). Thus the finding that the main viral structural proteins relocalise specifically in response to cytoskeletal disruption indicates that influenza virion assembly occurs at specific regions of the plasma membrane that are linked to the actin cytoskeleton. In addition, the matching redistribution of HA, M1, and NP after cytoskeletal disruption is consistent with the existence of interactions between these components that are involved in virion assembly. However, it does not rule out the possibility of additional or alternative independent interactions with a common cellular component, of which the actin aggregation at the center of the annuli is the most obvious candidate. Such a hypothesis is supported by the ability of NP to bind F-actin (Digard *et al.,* 1999, 2001) and it would be interesting to examine the behaviour of recombinant influenza viruses encoding NP mutants with defects in actin binding, if such viruses can be generated.

It is not self-evident why actin disruption and the formation of annuli should preclude the formation of filamentous but not spherical virions. Similar to others, we have found no convincing evidence for the incorporation of actin into viral filaments budding from cells. Not only do we see no significant staining of filaments with anti-β actin (Fig. 2a), we have been unable to consistently detect actin in filaments by staining with fluorescently labelled phalloidin, cytochalasin D, actin, or the actin-binding protein cofilin (data not shown). Equally, cytoskeletal disruption is not accompanied by any apparent gross defect in the transport of influenza virion components to the sites of virus assembly. Although we have not directly examined whether annuli also incorporate NA, M2, NEP/NS2, and the polymerase complex (because of the lack of suitable antibodies for the first two and the low abundance of the latter pair), the major internal virion components assemble at annuli (Figs. 5 and 6) and spherical virion assembly continues unaffected (Table 1, Fig. 4). Strains of influenza which produce predominantly spherical virions have previously been shown to bud from lipid raft domains in the plasma membrane, and several studies have investigated the requirements for HA and NA association with these domains (Scheiffele *et al.,* 1997, 1999; Keller and Simons, 1998; Barman and Nayak, 2000; Zhang *et al.,* 2000). Here, the study of influenza virus and its interactions with lipid raft domains was extended to the filamentous influenza virus A/Udorn/72. The HA protein of this virus was also found to be raft-incorporated, being insoluble in the nonionic detergent TX-100 at 4°C and present in DIGs following sucrose density gradient centrifugation (Figs. 5 and 7). In addition, filamentous virus particle production was inhibited by cholesterol depletion with the drug methyl-β-cyclodextrin at concentrations which did not prevent transport of HA to the cell surface (M. Simpson-Holley and P. Digard, unpublished data). We conclude that filamentous virus particles, similar to spherical viruses, bud from lipid raft domains in the plasma membrane. The annular domains seen after treatment with actin-disrupting drugs also showed characteristics typical of lipid rafts. Hence annuli also appear to be constructed from lipid rafts and this in turn supports the hypothesis that they correspond to aggregated viral budding domains.

The observation that the major structural polypeptides of influenza virus specifically redistribute in response to disruption of the cortical actin web provides further support for the prevalent hypothesis that lipid rafts interact with the actin cytoskeleton in a manner that controls their distribution. Previously, lipid rafts have been observed in single particle tracking experiments to behave as if tethered to an underlying structure, for which the membrane-associated cytoskeleton is an obvious candidate (Pralle *et al.,* 2000), while biochemical analysis of low-density DIG fractions often shows the presence of actin (Chang *et al.,* 1994; Dermine *et al.,* 2001). Several studies have shown that manipulation of raft-associated glycoproteins can lead to matching rearrangement of underlying microfilaments, particularly in the context of T cell signalling (Deckert *et al.,* 1996; Janes *et al.,* 1999; Harder and Simons, 1999; Oliferenko *et al.,* 1999; Roper *et al.,* 2000; Stahlhut and van Deurs, 2000; reviewed by Simons and Toomre, 2000). However, we are unaware of previous studies which show the converse, that manipulation of the actin cytoskeleton by a variety of drugs leads to the formation of a specific lipid-raft-containing structure on the cell surface.

The finding that lipid raft organisation is disrupted by cortical actin rearrangements in the presence of actin-disrupting drugs raises the possibility that this disruption is responsible for the loss of filamentous virus budding. The question remains though, of why the loss of normal raft organisation should specifically affect filamentous but not spherical virus assembly. Filamentous influenza virions are very large structures; quantification of the size of the filaments produced by the virus–cell combination used in this study indicated an average length of 11 ± 4 μm ($n = 102$). This is orders of magnitude larger than the estimated size of single lipid raft domains (Kenworthy and Edidin, 1998; Varma and Mayor, 1998; Pralle *et al.,* 2000; Schutz *et al.,* 2000) and far larger than any known examples of specialised raft assemblages yet described, such as caveolae (Harder and Simons, 1999; Kurzchalia

and Parton, 1999). Theoretically, at its simplest, the entire lipid envelope of a spherical virus particle of 100 nm diameter could be supplied by a single lipid raft of around 200 nm diameter, less than the mean size of the lipid domains measured by Schutz *et al.* (2000). However, a 10-μm-long viral filament has approximately 100 times the surface area of a similar diameter sphere, so the construction of a viral filament even partially composed of raft lipid would require a much larger number of raft domains. We therefore propose that the assembly of filamentous virions requires the actin cytoskeleton because filaments grow by incorporating multiple separate lipid raft domains and the mobility of HA-containing lipid rafts is subject to control by microfilaments. In this model, filamentous virion assembly fails after cytoskeletal disruption because the consequent aggregation of raft domains into annuli surrounding actin cores interferes with the serial recruitment of lipid rafts necessary to maintain filament growth. In contrast, the assembly of spherical virus particles remains unaffected because of the much smaller number of raft domains necessary for the formation of a single virus particle.

Interestingly, a recent study examining the budding morphology of human parainfluenza virus type 2 (HPIV-2) found that filament formation was inhibited by jasplakinolide or cytochalasin D treatment without significant effect on the overall titre of released virus at 24 h p.i. (Yao and Compans, 2000). The authors suggested that filamentous virion assembly requires the cytoskeleton to maintain cell polarity, a factor shown to be important for both influenza virus and HPIV-2 filament assembly (Roberts and Compans, 1998; Yao and Compans, 2000). However, jasplakinolide treatment induced the formation of small clumps of HPIV-2 surface antigens and although confocal microscopy was not used or actin distribution examined, it is possible these structures are equivalent to the HA annuli described here. To our knowledge, it is not known whether HPIV-2 utilises lipid rafts for budding: the hypothesis that the cytoskeleton controls and maintains the necessary raft dynamics for filamentous virion assembly predicts that it does.

MATERIALS AND METHODS

Cells, antibodies, and reagents

MDCK cells with a transepithelial electrical resistance of 800 Ω/cm^2 were used. Cells were grown on glass coverslips for immunofluorescence, AFM, and SEM, and on tissue culture plates for TEM and biochemical experiments. Cells were cultured in Dulbecco's modified Eagle's medium supplemented with L-glutamine, penicillin, streptomycin, and 10% foetal calf serum.

Rabbit antiserum to influenza virus recombinant A/X/31 (H3N2) was a kind gift of Dr. D. Steinhauer, NIMR, Mill Hill. This antiserum was used to stain for the extracellular viral proteins of Udorn virus and has been shown to detect mainly the haemagglutinin (data not shown). Rabbit polyclonal antibody to RNP has been previously described (Digard *et al.,* 1999). TRITC-conjugated phalloidin and anti-β-actin (clone AC-74) were purchased from Sigma. Jasplakinolide, latrunculin A, and anti-rabbit IgG antibodies conjugated to Alexa 594 were purchased from Molecular Probes Ltd. Cytochalasin D was purchased from Sigma-Aldrich Ltd. Drugs were dissolved in dimethylsulphoxide (DMSO) and DMSO included alone as a control in all experiments. Anti-rabbit and anti-mouse antibodies conjugated to FITC were purchased from DAKO.

Plasmid pGFPM703, encoding a GFP-M1 gene fusion under the control of a cytomegalovirus immediate early promoter, was constructed by cloning a cDNA copy of segment 7 from A/PR/8/34 (Young *et al.,* 1983) into plasmid pEGFP-C2 (Clontech). A product of the expected size (54 kDa) was detected by Western blot using anti-M1 and anti-GFP antibodies (data not shown).

Virus infections and transfections

Influenza virus A/Udorn/72 was a kind gift of Dr. R. Compans, Emory University, Atlanta (Roberts and Compans, 1998). The virus was grown in MDCK cells in the presence of 1 μg/ml trypsin and 0.14% bovine serum albumin. The supernatant was clarified, titred by serial dilution on MDCK cells, and was stored at -70°C until use. The Cambridge line of A/PR/8/34 was propagated in embryonated eggs as previously described (Blok *et al.,* 1996; Elton *et al.,* 2001), titred, and stored as described above. Cell monolayers were washed with PBS and infected at a multiplicity of infection of 10 for 1 h at 37°C. Cells were then washed and incubated in medium in the presence or absence of drug as desired. At 8 h p.i. cells were fixed for microscopy or prepared for extraction of raft membranes as described below. Cells were transfected with plasmids (0.3 μg/10^5 cells) using Lipofectin (GIBCO-BRL) according to the manufacturer's instructions (Digard *et al.,* 1999).

Microscopy

For immunofluorescence, cells were washed in PBS, fixed with 4% formaldehyde in PBS at room temperature for 20 min, and washed with PBS containing 2% newborn calf serum (NCS). Cells were incubated with primary antibodies and bound antibody detected by use of appropriate fluorophore-conjugated secondary antibody (Digard *et al.,* 1999; Elton *et al.,* 2001). Coverslips were mounted in Prolong antifade reagent (Molecular Probes) and examined using a Leica TCS NT confocal microscope. To generate images of whole cells, serial optical planes of focus (at $\sim$0.5-μm intervals) were taken in the *z*-axis through the depth of the cell and merged into one image using the extended focus algorithm in the software package TCS-NT (Leica). *z*-Axis ("side-view") reconstructions were generated from similar serial optical

planes of focus taken through the depth of the cell using the orthogonal view algorithm in TCS-NT. Laser power and photomultiplier tube settings were kept identical between matching samples stained with the same antibody. For SEM, cells were washed in 0.1 M HEPES pH 7.4, 2 mM $CaCl_2$ and fixed overnight in the same buffer containing 0.3% H_2O_2 and 4% EM-grade glutaraldehyde (Sigma; HEPES–glutaraldehyde). Cells were washed, fixed again in 1% osmium tetroxide, and dehydrated in serial alcohol dilutions. Samples were dried in a Polaron E 3000 critical point drier, sputter coated with AuPd to a thickness of 5 nm using a Polaron E5000, and viewed under a Philips XL 30 FEG SEM. For AFM, cells were fixed with glutaraldehyde as described for SEM, washed with distilled water, and air dried. Samples were observed using a Digital Instruments MultiMode AFM under the control of a Nanoscope IIIa controller. Digital Instruments Nanoprobe AFM tips (spring constant of 0.38 N/m) were used for contact-mode imaging. For TEM, monolayers of cells grown in 5-cm tissue culture dishes were washed in 0.1 M HEPES pH 7.4. The monolayer was then covered in HEPES–glutaraldehyde and left at 4°C for 1.5 h. The monolayer was then washed with HEPES buffer and cells scraped into buffer and harvested by centrifugation at 13,000 rpm for 10 min. The supernatant was then replaced with fresh HEPES buffer and sent to Cambridge University Multi-Imaging Centre, Department of Anatomy, for further fixation and sectioning.

Isolation of glycosphingolipid-rich TX100-insoluble membrane fractions

Confluent cell monolayers were washed twice (on ice at 4°C) with ice-cold PBS and overlaid with 1% TX100 in 25 mM Tris pH 7.5, 150 mM NaCl, 15 mM EDTA (TNE) (Manie *et al.,* 2000) on ice for 30 min. The cells were then scraped off and the suspension adjusted to 40% sucrose in TNE. Samples were transferred to centrifuge tubes and overlaid with steps of 30 and 4% sucrose in TNE. Gradients were spun at 36,000 rpm in a Beckmann SW55 rotor for 16 h at 4°C. Fractions were collected from the bottom of centrifuge tubes and analysed by Western blotting. Secondary antibodies conjugated to horseradish peroxidase were used (DAKO) and bound antibody detected by chemiluminescence (ECL reagent, Amersham). Luminescence was quantified using an Alpha Innotech Corporation Multi-Image cabinet according to the manufacturer's instructions.

ACKNOWLEDGMENTS

We thank Roger Hallam for constructing plasmid pGFPM703, Drs. Robert Henderson and Mike Edwardson for help with AFM, and Drs. Wendy Barclay, Amanda Stuart, and Vassilis Koronakis for helpful discussion. We also thank Tony Burgess for work on the SEM. This work was supported by grants from the Royal Society and Wellcome Trust (059151) to P.D. P.D. is a Royal Society University Research Fellow. M.S.-H. was supported by a BBSRC CASE studentship.

REFERENCES

Ali, A., Avalos, R. T., Ponimaskin, E., and Nayak, D. P. (2000). Influenza virus assembly: Effect of influenza virus glycoproteins on the membrane association of M1 protein. *J. Virol.* **74,** 8709–8719.

Avalos, R. T., Yu, Z., and Nayak, D. P. (1997). Association of influenza virus NP and M1 proteins with cellular cytoskeletal elements in influenza virus-infected cells. *J. Virol.* **71,** 2947–2958.

Bachi, T., Gerhard, W., Lindermann, J., and Muhlethaler, K. (1969). Morphogenesis of influenza A virus in Ehrlich ascites tumor cells as revealed by thin sectioning and freeze-etching. *J. Virol.* **4,** 769–776.

Barman, S., and Nayak, D. (2000). Analysis of the transmembrane domain of influenza virus neuraminidase, a type II transmembrane glycoprotein, for apical sorting and raft association. *J. Virol.* **74,** 6538–6545.

Benting, J., Rietveld, A. G., Ansorge, I., and Simons, K. (1999). Acyl and alkyl chain length of GPI-anchors is critical for raft association *in vitro. FEBS Lett.* **462,** 47–50.

Blok, V., Cianci, C., Tibbles, K. W., Inglis, S. C., Krystal, M., and Digard, P. (1996). Inhibition of the influenza virus RNA-dependent RNA polymerase by antisera directed against the carboxy-terminal region of the PB2 subunit. *J. Gen. Virol.* **77,** 1025–1033.

Bohn, W., Mannweiler, K., Hohenberg, H., and Rutter, G. (1987). Replica-immunogold technique applied to studies on measles virus morphogenesis. *Microscopy* **1,** 319–330.

Brown, D. A., and London, E. (1998). Functions of lipid rafts in biological membranes. *Annu. Rev. Cell Dev. Biol.* **14,** 111–136.

Brown, D. A., and London, E. (2000). Structure and function of sphingolipid and cholesterol rich membrane rafts. *J. Biol. Chem.* **275,** 17221–17224.

Brown, D. A., and Rose, J. K. (1992). Sorting of GPI-anchored proteins to glycolipid-enriched membrane subdomains during transport to the apical cell surface. *Cell* **68,** 533–544.

Bubb, M. R., Senderowicz, A. M., Sausville, E. A., Duncan, K. L., and Korn, E. D. (1994). Jasplakinolide, a cytotoxic natural product, induces actin polymerisation and competitively inhibits the binding of phalloidin to F-actin. *J. Biol. Chem.* **269,** 14869–14871.

Bubb, M. R., Spector, I., Beyer, B. B., and Fosen, K. M. (2000). Effects of jasplakinolide on the kinetics of actin polymerization. An explanation for certain *in vivo* observations. *J. Biol. Chem.* **275,** 5163–5170.

Chang, W. J., Ying, Y. S., Rothberg, K. G., Hooper, N. M., Turner, A. J., Gambliel, H. A., De Gunzburg, J., Mumby, S. M., Gilman, A. G., and Anderson, R. G. (1994). Purification and characterization of smooth muscle cell caveolae. *J. Cell Biol.* **126,** 127–138.

Choppin, P. W., Murphy, J. S., and Tamm, I. (1960). Studies of two kinds of virus particles which comprise influenza A2 virus strains. *J. Exp. Med.* **112,** 945–952.

Chu, C. M., Dawson, I. M., and Elford, W. J. (1949). Filamentous forms associated with newly isolated influenza virus. *Lancet* **1,** 602–605.

Compans, R. W., and Choppin, P. W. (1975). Reproduction of myxoviruses. *In* "Comprehensive Virology" (Fraenkel-Conrat H., Wagner R. R., Eds.), Vol. IV, pp. 179–252. Plenum, New York.

Coue, M., Brenner, S. L., Spector, I., and Korn, E. D. (1987). Inhibition of actin polymerisation by latrunculin A. *FEBS Lett.* **213,** 316–318.

Deckert, M., Ticchioni, M., and Bernard, A. (1996). Endocytosis of GPI-anchored proteins in human lymphocytes: Role of glycolipid-based domains, actin cytoskeleton, and protein kinases. *J. Cell Biol.* **133,** 791–799.

Dermine, J.-F., Duclos, S., Garin, J., St-Louis, F., Rea, S., Parton, R. G., and Desjardins, M. (2001). Flotillin-1-enriched lipid raft domains accumulate on maturing phagosomes. *J. Biol. Chem.* **276,** 18507–18512.

Digard, P., Elton, D., Bishop, K., Medcalf, E., Weeds, A., and Pope, B. (1999). Modulation of the nuclear localization of the influenza virus nucleoprotein through interaction with actin filaments. *J. Virol.* **73,** 2222–2231.

Digard, P., Elton, D., Simpson-Holley, M., and Medcalf, E. (2001). Interaction of the influenza virus nucleoprotein with F-actin. *In* "Options for

the Control of Influenza IV. International Congress Series," Vol. 1219, pp. 503–512. Elsevier Biomedical Press, Holland.

Elton, D., Simpson-Holley, M., Archer, K., Medcalf, E., McCauley, J., and Digard, P. (2001). Interaction of the influenza virus nucleoprotein with the cellular CRM1-mediated nuclear export pathway. *J. Virol.* **75,** 408–419.

Enami, M., and Enami, K. (1996). Influenza virus haemagglutinin and neuraminidase glycoproteins stimulate the membrane association of the matrix protein. *J. Virol.* **70,** 6653–6657.

Fiedler, K., Kobayashi, T., Kurzchalia, T. V., and Simons, K. (1993). Glycosphingolipid-enriched, detergent insoluble complexes in protein sorting in epithelial cells. *Biochemistry* **32,** 6365–6373.

Friedrichson, T., and Kurzchalia, T. V. (1998). Microdomains of GPI-anchored proteins in living cells revealed by crosslinking. *Nature* **394,** 802–805.

Griffin, J. A., and Compans, R. W. (1979). Effect of cytochalasin B on the maturation of enveloped viruses. *J. Exp. Med.* **150,** 379–391.

Harder, T., Scheiffele, P., Verkade, P., and Simons, K. (1998). Lipid domain structure of the plasma membrane revealed by patching of membrane components. *J. Cell Biol.* **141,** 929–942.

Harder, T., and Simons, K. (1999). Clusters of glycolipid and glycosphosphatidylinositol-anchored proteins in lymphoid cells: Accumulation of actin regulated by local tyrosine phosphorylation. *Eur. J. Immunol.* **29,** 556–562.

Husain, M., and Gupta, C. M. (1997). Interactions of viral matrix protein and nucleoprotein with the host cell cytoskeletal actin in influenza viral infection. *Curr. Sci.* **73,** 40–47.

Jacobson, K., and Dietrich, C. (1999). Looking at lipid rafts? *Trends Cell Biol.* **9,** 87–91.

Janes, P. W., Ley, S. C., and Magee, A. I. (1999). Aggregation of lipid rafts accompanies signalling via the T-cell receptor. *J. Cell Biol.* **147,** 447–461.

Jin, H., Leser, G. P., Zhang, J., and Lamb, R. A. (1997). Influenza virus hemagglutinin and neuraminidase cytoplasmic tails control particle shape. *EMBO J.* **16,** 1236–1247.

Keller, P., and Simons, K. (1998). Cholesterol is required for the surface transport of influenza virus haemagglutinin. *J. Cell Biol.* **140,** 1357–1367.

Kenworthy, A. K., and Edidin, M. (1998). Distribution of a glycosylphosphatidylinositol-anchored protein at the apical surface of MDCK cells examined at a resolution of 100 A using imaging fluorescence resonance energy transfer. *J. Cell. Biol.* **142,** 69–84.

Kurzchalia, T. V., and Parton, R. G. (1999). Membrane microdomains and caveolae. *Curr. Opin. Cell Biol.* **11,** 424–431.

Lamb, R. A., and Krug, R. M. (1996). Orthomyxoviridae: The viruses and their replication. *In* "Fields Virology" (B. N. Fields, D. M. Knipe, P. M. Howley, Eds.), pp. 1177–1204. Lippincott-Raven, Philadelphia.

Manie, S. N., Debreyne, S., Vincent, S., and Gerlier, D. (2000). Measles virus structural components are enriched into lipid raft microdomains: A potential cellular location for virus assembly. *J. Virol.* **74,** 305–311.

Martin, K., and Helenius, A. (1991). Transport of incoming influenza virus nucleocapsids into the nucleus. *J. Virol.* **65,** 232–244.

Mosley, V. M., and Wyckoff, R. W. G. (1946). Electron micrography of the virus of influenza. *Nature* **157,** 263.

Naim, H. Y., and Roth, M. G. (1993). Basis for the selective incorporation of glycoproteins into the influenza virus envelope. *J. Virol.* **67,** 4831–4841.

Oliferenko, S., Paiha, K., Harder, T., Gerke, V., Schwarzler, C., Schwarz, H., Beug, H., Gunthert, U., and Huber, L. A. (1999). Analysis of CD44-containing lipid rafts: Recruitment of annexin II and stabilization by the actin cytoskeleton. *J. Cell Biol.* **146,** 843–854.

O'Neill, R. E., Talon, J., and Palese, P. (1998). The influenza virus NEP (NS2 protein) mediates the nuclear export of viral ribonucleoproteins. *EMBO J.* **17,** 288–296.

Portela, A., and Digard, P. (2002). The influenza virus nucleoprotein: A multifunctional RNA-binding protein pivotal to virus replication. *J. Gen. Virol.* **83,** 723–734.

Pralle, A., Keller, P., Florin, E. L., Simons, K., and Horber, J. K. (2000). Sphingolipid-cholesterol rafts diffuse as small entities in the plasma membrane of mammalian cells. *J. Cell Biol.* **148,** 997–1007.

Rindler, M. J., Ivanov, I. E., Plesken, H., and Sabatini, D. D. (1985). Polarized delivery of viral glycoproteins to the apical and basolateral plasma membranes of Madin-Darby canine kidney cells infected with temperature-sensitive viruses. *J. Cell Biol.* **100,** 136–151.

Roberts, P. C., and Compans, R. W. (1998). Host cell dependence of viral morphology. *Proc. Natl. Acad. Sci. USA* **95,** 5746–5751.

Roberts, P. C., Lamb, R. A., and Compans, R. W. (1998). The M1 and M2 proteins of influenza virus are important determinants in filamentous particle formation. *Virology* **240,** 127–137, doi:10.1006/viro.1997.8916.

Roper, K., Corbeil, D., and Huttner, W. B. (2000). Retention of prominin in microvilli reveals distinct cholesterol-based lipid microdomains in the apical plasma membrane. *Nat. Cell Biol.* **2,** 582–592.

Ruigrok, R. W. H., Krugsman, F. M., De Ronde-Verloop, F. M., and De Jong, J. C. (1985). Natural heterogeneity of shape, infectivity and protein composition in an influenza A (H3N2) virus preparation. *Virus Res.* **3,** 69–76.

Scheiffele, P., Rietveld, A., Wilk, T., and Simons, K. (1999). Influenza viruses select ordered lipid domains during budding from the plasma membrane. *J. Biol. Chem.* **274,** 2038–2044.

Scheiffele, P., Roth, M. G., and Simons, K. (1997). Interaction of influenza virus haemagglutinin with sphingolipid-cholesterol membrane domains via the transmembrane domain. *EMBO J.* **16,** 5501–5508.

Schliwa, M. (1982). Action of cytochalasin D on cytoskeletal networks. *Cell* **92,** 79–91.

Schutz, G. J., Kada, G., Pastushenko, V. P., and Schindler, H. (2000). Properties of lipid microdomains in a muscle cell membrane visualized by single molecule microscopy. *EMBO J.* **19,** 892–901.

Simons, K., and Ikonen, E. (1997). Functional rafts in cell membranes. *Nature* **387,** 569–572.

Simons, K., and Toomre, D. (2000). Lipid rafts and signal transduction. *Nat. Rev.* **1,** 31–39.

Smirnov, I. A. (1991). The genetic aspects of influenza virus filamentous particle formation. *Arch. Virol.* **118,** 279–284.

Stahlhut, M., and van Deurs, B. (2000). Identification of filamin as a novel ligand for caveolin-1: Evidence for the organization of caveolin-1-associated membrane domains by the actin cytoskeleton. *Mol. Biol. Cell* **11,** 325–337.

Van Meer, G., and Simons, K. (1982). Viruses budding from either the apical or the basolateral plasma membrane domain of MDCK cells have unique phospholipid compositions. *EMBO J.* **1,** 847–852.

Varma, R., and Mayor, S. (1998). GPI-anchored proteins are organized in submicron domains at the cell surface. *Nature* **394,** 798–801.

Wehland, J., Osborn, M., and Weber, K. (1977). Phalloidin-induced actin polymerisation in the cytoplasm of cultured cells interferes with cell locomotion and growth. *Proc. Natl. Acad. Sci. USA* **74,** 5613–5617.

Yao, Q., and Compans, R. W. (2000). Filamentous particle formation by human parainfluenza virus type 2. *J. Gen. Virol.* **81,** 1305–1312.

Ye, Z., Liu, T., Offringa, D. P., McInnis, J., and Levandowski, R. A. (1999). Association of influenza virus matrix protein with ribonucleoproteins. *J. Virol.* **73,** 7467–7473.

Ye, Z., Robinson, D., and Wagner, R. R. (1995). Nucleus-targeting domain of the matrix protein (M1) of influenza virus. *J. Virol.* **69,** 1964–1970.

Young, J. F., Desselberger, U., Graves, P., Palese, P., Shatzman, A., and Rosenberg, M. (1983). Cloning and expression of influenza virus genes. *In* "The Origin of Pandemic Influenza Viruses" (W. G. Laver, Ed.), pp. 129–138. Elsevier Science, Amsterdam.

Zhang, J., and Lamb, R. A. (1996). Characterization of the membrane association of the influenza virus matrix protein in living cells. *Virology* **225,** 255–265, doi:10.1006/viro.1996.0599.

Zhang, J., Pekosz, A., and Lamb, R. A. (2000). Influenza virus assembly and lipid raft microdomains: A role for the cytoplasmic tails of the spike glycoproteins. *J. Virol.* **74,** 4634–4644.

Zvonarjev, A. Y., and Ghendon, Y. Z. (1980). Influence of membrane (M) protein on influenza A virus virion transcriptase activity *in vitro* and its susceptibility to rimantadine. *J. Virol.* **33,** 583–586.